

Multiple anomaly ranges in a shoulder-dumbbell system

Alan Barros de Oliveira^{1,2}, Eduardo B. Neves³, Cristina Gavazzoni²,

Juliana Z. Paukowski², Paulo A. Netz⁴, Marcia C. Barbosa²

¹ *Departamento de Física, Universidade Federal de Ouro Preto, Ouro Preto, MG, 35400-000, Brazil*

² *Instituto de Física, Universidade Federal do Rio Grande do Sul, Porto Alegre, RS, 91501-970, Brazil.*

³ *Petrobrás, Av. Elias Agostinho, 665, OP-EN-Imbetiba, Macaé, RJ, 27913-350, Brazil.*

⁴ *Instituto de Química, Universidade Federal do Rio Grande do Sul, Porto Alegre, RS, 91501-970, Brazil.*

(Dated: December 24, 2018)

We report for the first time a system that exhibits two regions in the pressure-temperature phase diagram where dynamic anomalies are present. Using molecular dynamics simulations, thermodynamic, dynamic and structural properties of rigid dimeric particles interacting with a core-softened shoulder-like intermolecular potential were investigated. The competition between the two length scales present in the core-softened potential and the third scale imposed by the dimeric character of the potential leads to a richer phase-diagram when compared to the monomeric system. The dimeric system exhibit two regions in the pressure-temperature phase-diagram where the diffusion and density are anomalous. A structural anomaly region was also found, englobing the double ranged thermodynamic and dynamic anomalies.

One of the biggest challenges in the study of complex fluids is the search for a simple isotropic interaction potential suitable to reproduce the anomalous behavior present in water [1, 2], such as the existence of a temperature of maximum density, liquid-liquid phase transition or non-monotonic diffusion behavior with respect to isothermal pressure variation [3, 4].

The recently proposed core-softened shoulder potential [5, 6, 7] reproduces the density and diffusion anomalies. This potential can represent in an effective and orientation-averaged way the interaction between water pentamers [8] characterized by the presence of two structures: one open and one closed. Similarly, the thermodynamic and dynamic anomalies result from the competition between the two length scales associated with the open and closed structures. Consequently, this model supports the idea that a potential with two competing length scales can give rise to thermodynamic and dynamic anomalies [9, 10, 11, 12]. Simple pair potentials are particularly interesting because they are computationally cheaper than molecular models as well as amenable under analytical treatments. For example, the recent perturbation theory developed by Zhou [13] is highly promising on attacking these sort of potentials.

Given that a two length scales potential exhibit one region of anomalies, how can one build a potential exhibiting two distinct regions of anomalies in the pressure-temperature phase-diagram? The answer to this question would be particularly useful for technological purposes, especially if one of the regions could be located at high pressures, where most polymer mixtures are produced and where particles diffuse slowly making difficult to the chemical industry to produce plastic materials. If two length scales potential exhibits one region of thermodynamic anomalies, a simple three length scales isotropic potential could be a good candidate for exhibiting two regions with anomalies in the pressure-

temperature phase-diagram. However, this is not the case. The presence of many closely spaced length scales in a spherical symmetric potential leads to one region in the pressure-temperature phase-diagram with thermodynamic and dynamic anomalies [14] because actually only the smaller and the larger scales compete effectively. In order to introduce a third length scale that would in fact compete with the two other scales, one alternative is to break the isotropic symmetry of the potential by introducing diatomic molecules that would interact through a two length scales potential.

Obviously anisotropic systems are not only more complicated but the addition of an extra degree of freedom results in a richer phase-diagram. For instance, diatomic particles interacting through a Lennard-Jones potential [15] exhibit a solid phase that occupies higher pressures and temperatures in the pressure-temperature phase diagram. In the case of the solid phase, the diatomic particles exhibit two close-packed arrangements instead of one observed in the monoatomic Lennard-Jones [16].

Here, in order to test our assumption that a three anisotropic length scales potential exhibit two anomalous regions, we consider a set of $N/2$ dimeric molecules formed each by two spherical particles of diameter σ , linked rigidly in pairs with the distance λ between their centers of mass as depicted in figure 1. Each particle within a dimer interacts with all particles belonging to other dimers with the intermolecular continuous shoulder potential [6] given by

$$U^*(r) = 4 \left[\left(\frac{\sigma}{r} \right)^{12} - \left(\frac{\sigma}{r} \right)^6 \right] + a \exp \left[-\frac{1}{c^2} \left(\frac{r - r_0}{\sigma} \right)^2 \right], \quad (1)$$

with the parameters: $a = 5.0$, $r_0/\sigma = 0.7$, $c = 1.0$ and $\lambda/\sigma = 0.2$.

We performed molecular dynamics simulations in the canonical ensemble using $N = 500$ particles (250 dimers)

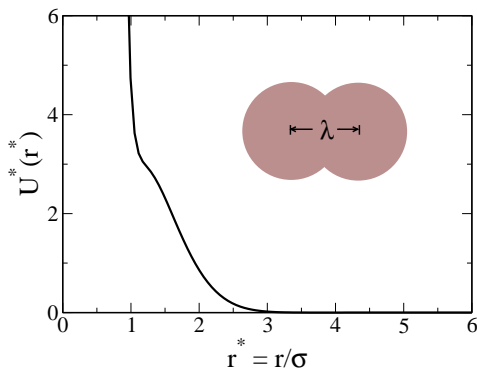


FIG. 1: Effective potential versus distance in reduced units.

in a cubic box with periodic boundary conditions, interacting with the intermolecular potential described above. The cutoff radius was set to 5.5σ . Pressure, temperature, density, and diffusion are calculated in dimensionless units, as detailed elsewhere [6].

Preliminary simulations showed that, depending on the chosen temperature and density, the system was in a fluid phase but became metastable with respect to the solid phase. In order to locate the phase boundary between the solid and the fluid phases two sets of simulations were carried out, one beginning with the molecules in an ordered crystal structure and the other beginning with the molecules in a random, liquid starting structure, obtained from previous equilibrium simulations. Thermodynamic and dynamic properties were calculated over 700 000 steps for the first set (and 900 000 steps for the second set), previously equilibrated over 200 000 (or 300 000) steps. The time step was 0.001 in reduced units, the time constant of the Berendsen thermostat [17] was 0.1 in reduced units. The internal bonds between the particles in each dimer remain fixed using the SHAKE [18] algorithm, with a tolerance of 10^{-12} and maximum of 100 interactions for each bond.

A broad range of temperatures ($0.10 \leq T^* \leq 3.00$) and densities ($0.10 \leq \rho^* \leq 0.60$) were simulated. The stability of the system was checked analyzing the dependence of pressure on density and also by visual analysis of the final structure, searching for cavitation. The structure of the system was characterized using the intermolecular radial distribution function, $g(r)$ (RDF), which does not take into account the correlation between atoms belonging to the same molecule. The diffusion coefficient was calculated using the slope of the least square fit to the linear part of the mean square displacement, $\langle r^2(t) \rangle$ (MSD), averaged over different time origins.

Fig. 2 shows (a) the pressure-temperature phase diagram of the system studied in this work, (b) the radial distribution functions, (c) the mean square displacements and, finally, (d) snapshots of the system at some interesting thermodynamic state points. The pressure-temperature phase diagram, illustrated in Fig. 2(a), dis-

plays a low density solid phase, a high density solid phase, a low density fluid phase, and a high density fluid phase. Near the boundaries of the high density solid phase, a liquid crystal-like phase was also identified, as discussed below. At intermediate temperatures as the pressure is isothermally increased (following the arrow in the figure 2 (a)) the system goes as follows: for low pressures the system is in the fluid phase, then as pressure increases it becomes solid, for higher pressures it becomes fluid again and then liquid crystal for even higher pressures. For very high pressures the system becomes solid again (not shown in the figure). The nature of the phases can be captured from the radial distribution function, from the mean square displacement, and from the snapshots.

While for $P^* = 1.17$ and 7.24 the system shows ordered structures, for $P^* = 0.194$ and 4.19 it presents no structure, what is typically characteristic of liquid or glass phase, depending on the mobility of particles in the system. According to the MSD, for $P^* = 0.194$ and $P^* = 4.19$ the particles show high mobility, whereas for $P^* = 1.17$ the particles do not move. This would be already expected from the corresponding RDFs. However for $P^* = 7.24$, the particles move almost as fast as in a liquid phase, but the corresponding RDF is rather solid-like. Which type of phase could be present in $P^* = 7.24$? In order to answer this question a movie with the evolution of the configurations was made. This movie is available as supplementary material and it shows that in this case the particles actually move, but only in a string-like fashion, what characterizes a liquid crystal-like phase.

The complete reduced pressure versus reduced temperature phase diagram of the system is illustrated in Fig. 3(a) and a zoom in of the high pressure region of the phase diagram is shown in Fig. 3(b). The *region of density anomaly*, bounded by the line of the temperatures of maximum density (TMD), was determined plotting the pressure against the temperature along isochors and locating the minima. For the model studied in this work, we have found two TMD lines, a low pressure-TMD and a high pressure-TMD line. The low pressure-TMD line is located between $2.0 < P^* < 3.5$, and the high pressure-TMD line is located for pressures in the range $6 < P^* < 8$. The former is shown in the Fig. 3(a) as a continuous bold line while the latter is represented as filled circles connected by a bold line. See the Fig. 3(b) for better visualization.

The *region of the dynamic anomaly* was obtained by computing the slope of the mean square displacement as a function of time. Figure 4 illustrates the diffusion coefficient as a function of density. For $T^* > 0.65$, the diffusion coefficient exhibits three regimes:

- (i) For low densities, $\rho < \rho_{D\min}$, D decreases as ρ increases as expected for normal fluids.
- (ii) For intermediate densities, i.e., inside the dotted ellipse, $\rho_{D\min} < \rho < \rho_{D\max}$, and D increases with density – an anomalous behavior, defining the region of dynamic

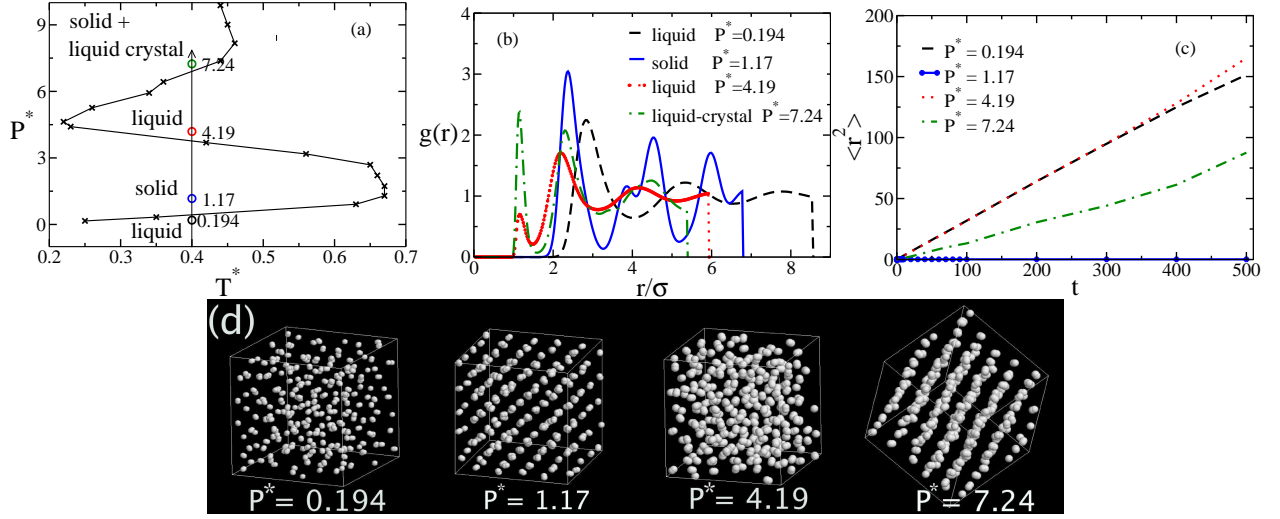


FIG. 2: (a) Reduced pressure versus reduced temperature phase-diagram showing the liquid and solid phases. The arrow at $T^* = 0.4$ crosses the regions with $P^* = 0.194, 1.17, 4.19$, and 7.24 illustrated in the radial distribution function. (b) Radial distribution function versus reduced distance for $T^* = 0.4$ and $P^* = 0.194, 1.17, 4.19$, and 7.24 . (c) Mean square displacement versus time for the four regions illustrated in (a): fluid, solid, fluid, and liquid crystal. With the slope of the MSD versus time for $P^* = 0.194, 1.17, 4.19, 7.24$ we calculate the diffusion coefficient that is zero for $P^* = 1.17$. (d) Snapshots of the configurations for $T^* = 0.4$ and the same pressures as in panel (a).

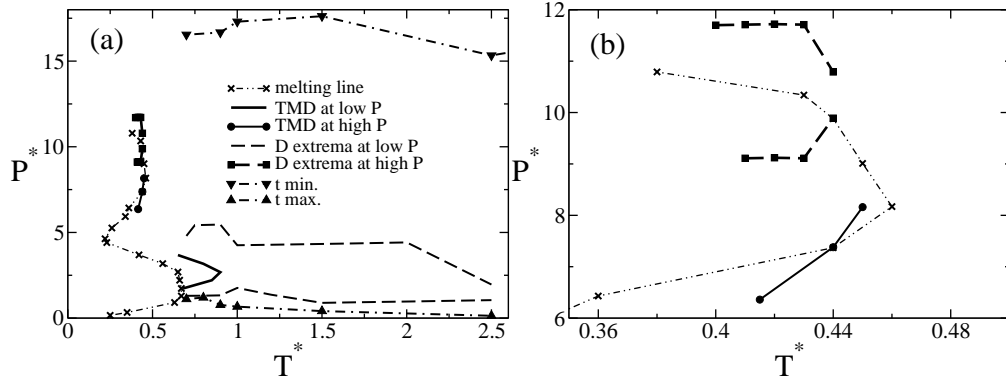


FIG. 3: (a) Pressure versus temperature phase diagram for dimeric particles interacting through the potential illustrated in Fig. 1 and (b) the zoom in of the region of high pressures of the phase-diagram.

anomalies.

(iii) For high densities, $\rho > \rho_{Dmax}$, the normal behavior is restored with D decreasing as density increases.

For each temperature there is a ρ_{Dmin} and a ρ_{Dmax} and consequently a $P_{Dmin}(T)$ and a $P_{Dmax}(T)$. The lines of $P_{Dmax}(T)$ and $P_{Dmin}(T)$ in the P - T phase diagram illustrated in Figure 3 are similar to the diffusivity extrema observed in experiments for water as well as in simulations of water [3, 4, 19], silica, [20, 21, 22], other isotropic potentials [23, 24, 25] and for the potential Fig. 1 with monomeric particles [6]. The region of diffusion anomaly in the P^* - T^* phase diagram is bounded by $P_{Dmin}(T)$ and $P_{Dmax}(T)$ and encloses the region of density anomaly, showing the same hierarchy found in water[4].

One of the most remarkable features in this system, however, is the existence of a second region of diffusion

anomaly. In the vicinity of the high density solid the region also exhibits the anomalous behavior illustrated in Fig. 4 (inside the dashed ellipse). The lines of $P_{Dmax}(T)$ and $P_{Dmin}(T)$ in the P - T phase diagram are illustrated in Figure 3. This second region of diffusion anomaly occupies a small region in the the P - T phase diagram at high pressure. See the zoom in of the high pressure region of the phase-diagram in the Fig. 3(b). The relation between this second diffusion anomaly region and the second density anomaly region is not hierarchical as in the case of the low-pressure anomalous regions discussed previously.

Besides the density and diffusion anomalies, the dimeric model analyzed in this work also presents structural anomaly, that is a decreasing of the order of the system upon compression. For measuring the order of the system we have used the so called translational or-

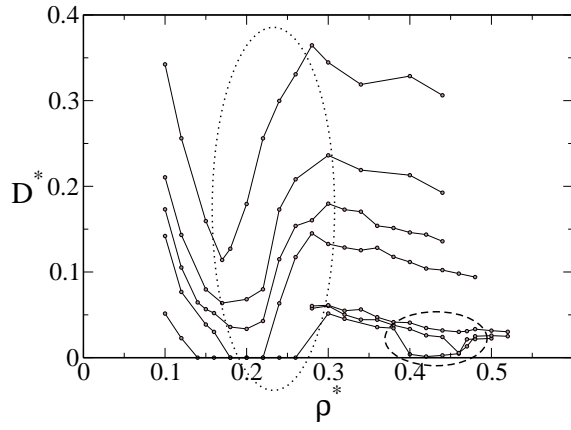


FIG. 4: Diffusion coefficient versus density at fixed temperatures, which are $T^* = 0.40, 0.42, 0.44, 0.65, 0.75, 0.90$, and 1.20 from bottom to top. The dotted ellipse roughly englobes the region where particles moves faster under compression at low P , while dashed ellipse marks the region where this effect appears at high pressures.

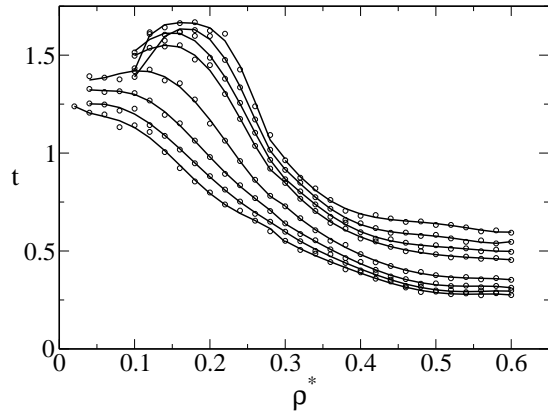


FIG. 5: Translational order parameter against density for fixed temperatures, which are $T^* = 0.7, 0.8, 0.9, 1.0, 1.5, 2.0, 2.5$, and 3.0 from top to bottom.

der parameter, t , calculated by means of the RDF [4, 7]. We have considered the structural anomaly region as the region where the translational order parameter decreases with density – or equivalently with compression. The results we have found are shown in Fig. 5. The region of structural anomaly is shown in Fig. 3(a) as the region between triangles-up and -down symbols.

In summary, we have found for the first time a potential with two anomalous regions. Unlike the monomeric system that exhibit just one region of density, diffusion, and structural anomalies, the dimeric system has two regions of anomalies. The reason for the appearance of the second region is related to the presence of three different structures competing at the solid phase: two solid phases and liquid-crystal phase. In that sense the first anomalous region appears as the result of the competi-

tion between one length scale (related to the low density solid phase) and the ordering in one plane (liquid crystal phase) and the other anomalous region emerges as the result of the competition between the liquid-crystal phase and the other length scale (related to the high density solid phase).

-
- [1] P. G. Debenedetti, F. Sciortino, and H. E. Stanley, *Phys. Rev. E* **53**, 6144 (1996).
 - [2] O. Mishima and H. E. Stanley, *Nature (London)* **396**, 329 (1998).
 - [3] P. A. Netz, F. W. Starr, H. E. Stanley, and M. C. Barbosa, *J. Chem. Phys.* **115**, 344 (2001).
 - [4] J. R. Errington and P. D. Debenedetti, *Nature (London)* **409**, 318 (2001).
 - [5] C. H. Cho, S. Singh, and G. W. Robinson, *Faraday Discuss.* **103**, 19 (1996).
 - [6] A. B. de Oliveira, P. A. Netz, T. Colla, and M. C. Barbosa, *J. Chem. Phys.* **124**, 084505 (2006).
 - [7] A. B. de Oliveira, P. A. Netz, T. Colla, and M. C. Barbosa, *J. Chem. Phys.* **125**, 124503 (2006).
 - [8] W. P. Krekelberg, J. Mittal, V. Ganesan, and M. Truskett, *Phys. Rev. E* **77**, 041201 (2008).
 - [9] A. B. de Oliveira, G. Franzese, P. A. Netz, and M. C. Barbosa, *Journal of Chemical Physics* **128**, 064901 (2008).
 - [10] A. B. de Oliveira, P. A. Netz, and M. C. Barbosa, *Europhysics Letters* **85**, 36001 (2009).
 - [11] P. Kumar, G. Franzese, and H. E. Stanley, *Phys. Rev. E* **73**, 041505 (2006).
 - [12] G. Franzese and H. E. Stanley, *J. Phys.: Cond. Matter* **19**, 205126 (2007).
 - [13] S. Zhou, *J. Chem. Phys.* **130**, 054103 (2009).
 - [14] P. A. Netz, S. Buldyrev, M. C. Barbosa, and H. E. Stanley, *Physical Review E* **73**, 061504 (2006).
 - [15] C. Kriebel and J. Winkelmann, *J. Chem. Phys.* **105**, 9316 (1996).
 - [16] C. Vega, C. McBride, E. de Mibuel, B. F. J., and A. Galindo, *J. Chem. Phys.* **118**, 10696 (2003).
 - [17] H. J. C. Berendsen, J. P. M. Postuma, W. F. van Gunsteren, A. DiNola, and J. R. Haak, *J. Chem. Phys.* **81**, 3684 (1984).
 - [18] J. P. Ryckaert, G. Ciccotti, and H. J. C. Berendsen, *J. Comput. Phys.* **23**, 327 (1977).
 - [19] J. Mittal, J. R. Errington, and T. M. Truskett, *J. Phys. Chem. B* **110**, 18147 (2006).
 - [20] P. H. Poole, M. Hemmati, and C. A. Angell, *Phys. Rev. Lett.* **79**, 2281 (1997).
 - [21] R. Sharma, A. Mudi, and C. Chakravarty, *J. Chem. Phys.* **125**, 044705 (2006).
 - [22] M. S. Shell, P. G. Debenedetti, and A. Z. Panagiotopoulos, *Phys. Rev. E* **66**, 011202 (2002).
 - [23] L. Xu, S. Buldyrev, C. A. Angell, and H. E. Stanley, *Phys. Rev. E* **74**, 031108 (2006).
 - [24] Z. Yan, S. V. Buldyrev, N. Giovambattista, and H. E. Stanley, *Phys. Rev. Lett.* **95**, 130604 (2005).
 - [25] Z. Yan, S. V. Buldyrev, N. Giovambattista, P. G. Debenedetti, and H. E. Stanley, *Phys. Rev. E* **73**, 051204 (2006).